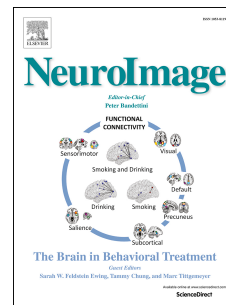


Journal Pre-proof

Attentional Modulation of the Auditory Steady-State Response across the Cortex

Cassia Low Manting, Lau M. Andersen, Balazs Gulyas, Fredrik Ullén, Daniel Lundqvist



PII: S1053-8119(20)30416-X

DOI: <https://doi.org/10.1016/j.neuroimage.2020.116930>

Reference: YNIMG 116930

To appear in: *NeuroImage*

Received Date: 15 October 2019

Revised Date: 10 April 2020

Accepted Date: 7 May 2020

Please cite this article as: Manting, C.L., Andersen, L.M., Gulyas, B., Ullén, F., Lundqvist, D., Attentional Modulation of the Auditory Steady-State Response across the Cortex, *NeuroImage*, <https://doi.org/10.1016/j.neuroimage.2020.116930>.

This is a PDF file of an article that has undergone enhancements after acceptance, such as the addition of a cover page and metadata, and formatting for readability, but it is not yet the definitive version of record. This version will undergo additional copyediting, typesetting and review before it is published in its final form, but we are providing this version to give early visibility of the article. Please note that, during the production process, errors may be discovered which could affect the content, and all legal disclaimers that apply to the journal pertain.

© 2020 Published by Elsevier Inc.

Attentional Modulation of the Auditory Steady-State Response across the Cortex

Cassia Low Manting^{1,2*}, Lau M. Andersen^{1,3}, Balazs Gulyas^{2,4}, Fredrik Ullén⁵ and Daniel Lundqvist¹

¹ NatMEG, Department of Clinical Neuroscience, Karolinska Institutet, Stockholm, Sweden

² Cognitive Neuroimaging Centre (CoNiC), Lee Kong Chien School of Medicine, Nanyang Technological University, Singapore

³ Center of Functionally Integrative Neuroscience, Aarhus University, Aarhus, Denmark

⁴ Department of Clinical Neuroscience, Karolinska Institutet, Stockholm, Sweden

⁵ Department of Neuroscience, Karolinska Institutet, Stockholm, Sweden

* corresponding author

E-mail: mtlow1@e.ntu.edu.sg, cassia@natmeg.se

Keywords

ASSR, frequency-tagging, selective auditory attention, amplitude-modulation, diotic, music

Abstract

Selective auditory attention allows us to focus on relevant sounds within noisy or complex auditory environments, and is essential for the processing of speech and music. The *auditory steady-state response (ASSR)* has been proposed as a neural measure for tracking selective auditory attention, even within continuous and complex soundscapes. However, the current literature is inconsistent on how the ASSR is influenced by selective attention, with findings based primarily on attention being directed to either ear rather than to sound content. In this experiment, a mixture of melody streams was presented to both ears identically (*diotically*) as we examined if selective auditory attention to sound content influences the ASSR. Using magnetoencephalography (MEG), we assessed the stream-specific ASSRs from three frequency-tagged melody streams when attention was directed between each melody stream, based on their respective pitch and timing. Our main results showed that selective attention enhances the ASSR power of an attended melody stream by 14 % at a general sensor level. This ability to readily capture attentional changes in a stimuli-precise manner makes the ASSR a useful tool for studying selective auditory attention, especially in complex auditory environments. As a secondary aim, we explored the distribution of cortical ASSR sources and their respective attentional modulation using a distributed source model of the ASSR activity. Notably, we uncovered the existence of ASSR attentional modulation outside the temporal cortices. Across-subject averages of the attentional enhancement over the cortical surface suggest that frontal regions show up to ~ 80 % enhancement, while temporal and parietal cortices were enhanced by 20 - 25 %. Importantly, this work advocates a novel ‘beyond the temporal cortex’ perspective on ASSR modulation and also serves as a template for future studies to precisely pin-point which cortical sites are more susceptible to ASSR attentional modulation.

1. Introduction

In light of the brain's limited capacity to process simultaneous information, the ability to attend to one out of several competing sounds is therefore essential, allowing one to extract and process the most important information amidst a complex auditory environment. This phenomenon was first coined the "Cocktail party effect (CPE)" by Cherry in 1953 and is important to functions such as speech recognition, musicianship and threat identification¹. In music, selective auditory attention can manifest as the ability to discern a single instrument in an orchestral performance, or a single voice in a choir. This ability, estimated with speech-in-noise performance² and robustness of neural patterns³, is positively correlated with the listener's amount of musical training²⁻³, suggesting that selective attention capabilities may be improved through strategic training regimes. While the relevance of the CPE for perception and performance is well documented, the neural mechanisms underlying this phenomenon are still not completely understood. This is partially due to the difficulties in isolating the specific brain activity that stem from one out of many simultaneous auditory sources: If you selectively attend to only the soprano voice while listening to a choir performance, how do you separate brain activity representing the soprano from that representing the rest of the choir and study how that activity is influenced by selective attention? Previous magnetoencephalography (MEG) and electroencephalography (EEG) studies on selective auditory attention have shown that time-locked neuronal activity [e.g. event-related fields (ERFs) and potentials (ERPs)] from a wide range of auditory stimuli (e.g. click, tones, speech) is increased by attention⁴⁻⁷. However, such time-locked approaches are not easily compatible with the complex and dynamic characteristics of naturalistic or continuous stimuli. Importantly, in a natural auditory environment sounds from different auditory sources often occur with approximately simultaneous onset times, and thus it is very difficult to distinguish such sounds from their event-related activities. In such scenarios, another approach using the Auditory Steady-State Response (ASSR) may be useful to isolate and assess the neural activity related to each individual sound.

The ASSR can be described as an oscillatory evoked potential that continuously phase-locks to the intrinsic fundamental frequency of the stimulus over the time period of stimulus presentation^{8,9}. The constituent discrete frequency components of the ASSR can be retrieved from recorded MEG/EEG data using power spectral density (PSD) estimation methods such as Fourier analysis. A handy way to adjust the stimulus frequency, and consequently the ASSR frequency, while retaining much of the stimulus property (e.g. pitch, timbre) is via *amplitude modulation (AM) frequency-tagging* of the sound. This is done by increasing and decreasing the amplitude of the sound envelope (i.e. volume) at a precise rate defined by the modulation frequency (f_m). This technique can be used to disentangle the processing of sound streams presented simultaneously, since the neural activity corresponding to each stream can be distinguished by a unique f_m during analysis¹⁰⁻¹¹. In humans, the ASSR is known to reach a maximum power response at frequencies close to 40 Hz⁹, hence the term *40 Hz ASSR*. Several intermodal studies have demonstrated that the cortically generated ASSR is enhanced when attention is voluntarily directed towards (as compared to directed away from) an auditory stimuli from a competing visual stimulus¹²⁻¹⁴. Within the auditory domain (i.e. intramodal studies) however, results remain unclear. In some cases, selective attention tasks using dichotic stimulus presentation reported an ASSR enhancement by attention while in other cases no effect of attention was found^{6, 15-17}. The inconsistency in findings suggests that whether or not attention is found to affect the ASSR depends on several experimental design factors pertaining to the stimuli, task and analytical approach. Furthermore, the majority of intramodal auditory attention ASSR studies adopt a *dichotic* experimental design wherein participants shift attention between the left and right ears, and the corresponding changes in cortical ASSRs are assessed with MEG^{15,18}. Therefore, selective attention in such dichotic experiments is heavily reliant on spatial separation of the auditory inputs to the two ears rather than perceptual separation of the sound streams based on sound content, despite the latter being an essential aspect of selective listening. Also, the spatial separation approach is inherently limited to two ears and thus only two sources, making it inapplicable to studies involving complex auditory mixtures with several sources. To the best of our knowledge, no study has examined the influence of selective attention on the 40 Hz ASSR when the same auditory mixture of multiple streams is presented to both ears (i.e. diotically), and auditory stream separation must be based solely on perceptual features of the sound content (i.e. pitch/timbre/tempo). This gap in the ASSR-attention literature may point to some challenges that researchers face in designing such an experiment, for example, in finding suitable stimuli and tasks with sufficient stream separability to evoke a detectable difference in selective attention when using diotic stimuli.

In the current study, we aim to explore this novel approach by using a task where selective attention is directed towards diotically-presented AM frequency-tagged melody streams that are easily differentiable by their respective timing and pitch. For the frequency-tagging, we used separate modulation frequencies at $f_m = 39, 41, 43$ Hz to individually tag each of three different melody streams, with the goal of eliciting ASSRs corresponding to the three melody streams that can be clearly separated in the frequency domain during analysis. To assess the ASSR, we measured ongoing brain activity at millisecond temporal resolution and millimetre spatial precision using MEG¹⁹. At the same time, MEG is also well-suited for spatially precise modelling of brain activity at an individual anatomical level.

The primary aim of this study was to assess if ASSR power is influenced when selective attention is directed towards a specific melody stream, and if this can be readily observed in sensor level MEG analyses. Based on the rich literature supporting the enhancement effect of selective attention on neural signals^{7, 20-23}, we hypothesized that attention increases the ASSR power corresponding to the attended stream. With sufficient signal power, we expect that this attention effect may be observed already in sensor-level data.

A secondary aim of this study is to gain insights into the structural distribution of the cortical sources that are involved in ASSR expression and their attentional modulation. Since little is known about the source distribution of the ASSR attentional

61 modulation, apart from its presence in the auditory cortex²⁴⁻²⁶, we have no specific *a priori* hypothesis about where to expect
 62 the ASSR attention effect, although attention-related literature does suggest the prefrontal cortex as a likely site²⁷⁻³⁰. Hence,
 63 we will first use a distributed source model to identify likely ASSR source positions, then statistically test whether there exist
 64 sources outside the auditory cortex that drive the attention effect. Furthermore, we will compute the across-subject average
 65 degree of attentional modulation in each of these ASSR source regions.

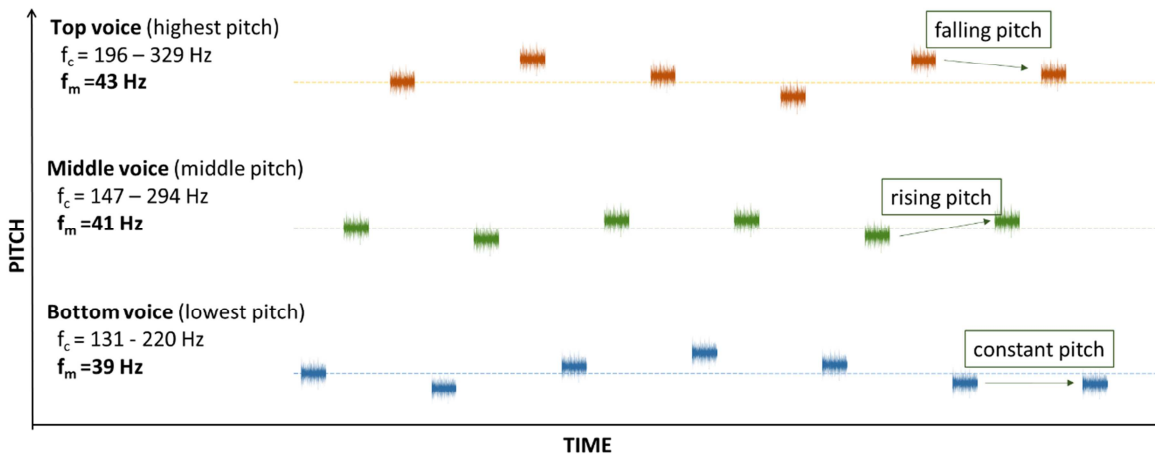
66 2. Materials and Methods

67 2.1 Participants

68 A total of 29 participants with normal hearing volunteered to take part in the experiment. The experiment was approved by
 69 the Regional Ethics Review Board in Stockholm (Dnr: 2017/998-31/2). Both written and oral informed consent were
 70 obtained from all participants prior to the experiment. All participants received a monetary compensation of SEK 600 (~ EUR
 71 60). One participant was excluded due to incomplete data collection, and a second participant was excluded due to less-than-
 72 chance performance in the behavioural task, resulting in a final sample size of 27 participants for all MEG analyses (age 18 –
 73 49 years, mean age = 28.6, SD = 6.2; 9 female; 2 left-handed).

74 2.2 Experimental Task: Melody Development Tracking (MDT) task

75 Participants were presented with 3 melody streams of increasing pitch [i.e. carrier frequency (f_c) range], henceforth
 76 referred to as the Bottom voice, Middle voice, and Top voice. The participants were instructed to direct attention exclusively
 77 to the Bottom voice or Top voice according to a cue before the melodies started (e.g. “Attend bottom voice!”). At a random
 78 surprise point during melody playback, the melody stopped and participants were asked to report the latest direction of pitch
 79 change for the attended melody stream by pressing one out of three buttons, representing *falling*, *rising* or *constant* pitch
 80 respectively (e.g. whether the last note was falling, rising or constant relative to the note preceding it. Refer to Fig. 1). In
 81 total, 28 of these responses were collected for each participant.



82
 83 **Figure 1.** The Melody Development Tracking (MDT) task. Participants listened to three melody streams while attending to either the
 84 Bottom voice or Top voice following a cue. When the melody stopped, participants were asked to report the last direction of pitch change
 85 for the attended melody stream (i.e. falling, rising or constant pitch as illustrated). The three melody streams were presented separately
 86 in time, starting from Bottom to Top (shown in figure) or its reverse. The respective f_c (pitch) range and f_m of each stream are indicated
 87 above.

88
 89 The three voices were presented separately in time, such that the voices had their note onset either in the order of Bottom-
 90 Middle-Top or its reverse, while keeping the order balanced across trials. Prior to the actual MEG recording, participants
 91 received 10 to 15 min of training to familiarize themselves with the task. Participants were deemed ready to commence with
 92 the actual experiment once they managed to report the correct answers for at least five consecutive trials. As the task was
 93 designed to require continuous selective attention to the cued melody stream, it was imperative to maintain alertness and
 94 alleviate fatigue. We therefore introduced a brief break in the task every ~5 min, during which the general attentiveness of the
 95 participant was also assessed using the Karolinska sleepiness scale³¹. To minimize movement artefacts, participants were
 96 asked not to move when listening to each melody segment, which was at most 30 s long. The MEG recording time was
 97 approximately 20 min per participant, including breaks.

98 2.3 Stimuli

99 Each of the three voices was constructed using a stream of 750 ms long sinusoidal tones of f_c between 131 – 329 Hz
 100 (Bottom voice: 131 - 220 Hz; Middle voice 147 – 294 Hz; Top voice 196 – 329 Hz), generated using the Ableton Live 9
 101 software (Berlin, Germany). At the onset and offset of each tone, we introduced a 25 ms amplitude fade-in and fade-out to
 102 avoid audible compression clicks. These tones were then amplitude-modulated sinusoidally in Ableton Live 9 using f_m at 39
 103 (Bottom voice), 41 (Middle voice), and 43 (Top voice) Hz, and a modulation depth of 100% to achieve maximum ASSR

power⁸. For simplicity, only tones in the C major harmonic scale were used. The duration of melody presentation was randomized to be between 9 – 30 seconds long to reduce predictability of the stop point and thereby maintain high attention throughout the melody. Loudness was calibrated using a soundmeter (Type 2235, Brüel & Kjær, Nærum, Denmark) to account for differences in subjective loudness for different frequency ranges³². The respective settings for the Bottom, Middle and Top voices were 0 dB, -6 dB and -10 dB. The stimulus was presented identically via ear tubes to both ears with the volume adjusted to be 75 dB SPL per ear, subjected to individual comfort level.

2.4 Data Acquisition

MEG measurements were carried out using a 306-channel whole-scalp neuromagnetometer system (Elekta TRIUX™, Elekta Neuromag Oy, Helsinki, Finland). Data was recorded at a 1 kHz sampling rate, on-line bandpass filtered between 0.1-330 Hz and stored for off-line analysis. Horizontal eye-movements and eye-blinks were monitored using horizontal and vertical bipolar electroculography electrodes. Cardiac activity was monitored with bipolar electrocardiography electrodes attached below the left and right clavicle. Internal active shielding was active during MEG recordings to suppress electromagnetic artefacts from the surrounding environment. In preparation for the MEG-measurement, each participant's head shape was digitized using a Polhemus FASTRAK. The participant's head position and head movement were monitored during MEG recordings using head-position indicator coils. Anatomical MRIs were acquired using hi-res Sagittal T1 weighted 3D IR-SPGR (inversion recovery spoiled gradient echo) images by a GE MR750 3 Tesla scanner with the following pulse sequence parameters: 1 mm isotropic resolution, FoV 240 × 240 mm, acquisition matrix: 240 × 240, 180 slices 1 mm thick, bandwidth per pixel=347 Hz/pixel, Flip Angle=12 degrees, TI=400 ms, TE=2.4 ms, TR=5.5 ms resulting in a TR per slice of 1390 ms.

2.5 Data Processing

The acquired MEG data was pre-processed using MaxFilter (-v2.2)³³⁻³⁴, and subsequently analysed and processed using the Fieldtrip toolbox³⁵ in MATLAB (Version 2016a, Mathworks Inc., Natick, MA), as well as the MNE-Python software³⁶. Cortical reconstruction and volumetric segmentation of all participants' MRI was performed with the Freesurfer image analysis suite³⁷.

2.5.1 Pre-Processing

MEG data was MaxFiltered by applying temporal signal space separation (tSSS) to suppress artefacts from outside the MEG helmet and to compensate for head movement during recordings³³⁻³⁴, before being transformed to a default head position. The tSSS had a buffer length of 10 s and a cut-off correlation coefficient of 0.98. The continuous MEG data was divided into 1 s-long epochs from stimulus onset (i.e. onset of each individual note). Epochs were then visually inspected for artefacts and outliers with high variance were rejected using *ft_rejectvisual*³⁵. After cleaning, the remaining 69 % of all epochs were kept for further analyses. The data was divided into six experimental conditions, consisting of epochs (~100 per condition) for each of the three voices (Bottom, Middle, Top) under instructions to attend the Bottom voice or Top voice, respectively, i.e.: i) Bottom voice – Attend Bottom (Bottom-Attend), ii) Bottom voice – Attend Top (Bottom-Unattend), iii) Top voice – Attend Top (Top-Attend), iv) Top voice – Attend Bottom (Top-Unattend), v) Middle voice – Attend Bottom, vi) Middle voice – Attend Top.

2.5.2 Behavioural data analysis

To assess response accuracy in the MDT task, mean task performance scores (number of correct responses out of 28 total responses) were calculated across all conditions separately for each participant.

2.5.3 Sensor-space analysis

We carried out sensor-space analysis on the cleaned MEG epochs to extract the effect of selective attention on the ASSR. ERFs were also extracted to check for the manipulation of attention by the task, since it has already been well-documented in literature that attention enhances the ERF⁴⁻⁷. For these analyses, firstly, a 30 – 50 Hz bandpass filter was applied to obtain the ASSR, and a 20 Hz low-pass filter was applied to obtain the ERF. Within each participant, the filtered epochs were then averaged per condition, resulting in the *timelocked ASSR* and *timelocked ERF*. The ERF data was demeaned using an interval, 100 - 0 ms before stimulus onset, as the baseline. To acquire the ASSR power spectrum in the frequency domain, a fast Fourier transform (hanning-tapered, frequency resolution = 1 Hz) was applied to the *timelocked ASSR* data above. The ASSR power spectrum and *timelocked ERF* data were further averaged across all gradiometer sensors, after collapsing data from orthogonal planar gradiometers, to give the average gradiometer data per participant. Gradiometer sensors were selected for analysis as they are generally less noisy compared to magnetometers. The ASSR power at f_m , (defined as 39, 41, and 43 Hz for the Bottom, Middle and Top voices respectively) was extracted accordingly for each of the six conditions to give the mean ASSR power at f_m per condition (e.g. For the Bottom-Attend and Bottom-Unattend conditions, the power at 39 Hz was used). To obtain the ERF sustained field amplitude per condition, the average amplitude across the *timelocked ERF* data was calculated using a 300 – 800 ms post-stimulus onset time window^{6, 38}.

2.5.4 Source-space analysis

158 In order to model the effect of selective attention on the ASSR at the anatomical level, we used a distributed source model
 159 containing 20484 dipolar sources on the cortical surface of each participant. By using a minimum-norm estimate (MNE)
 160 approach³⁶, we estimated the amplitude of these sources that generated the ASSR. The *timelocked* ASSR data was used for this
 161 analysis, to produce MNE solutions for each participant that were subsequently morphed to a common head template -
 162 fsaverage. As an initial step, we calculated the group-averaged morphed MNE solution before computing its power spectral
 163 density (PSD) using Welch's method (hanning windowed, frequency resolution = 1 Hz).

164 We then used the middle voice (excluded from source analyses addressing the attention effect on ASSR) PSD as a
 165 localizer to identify ASSR sources across the cortex. The entire cortical sheet was divided into 105 sub-regions per
 166 hemisphere according to the Brainnetome Atlas³⁹, and the PSDs of all vertices within each sub-region were averaged to give a
 167 median *localizer power* per sub-region. For the sake of clarity, we used the occipital lobe as a reference for the absence of
 168 strong and independent ASSR sources, and discarded 24 sub-regions (12 per hemisphere) with *localizer power* less than the
 169 mean *localizer power* across all vertices in the occipital lobe ($4.83 \cdot 10^{-27} \text{ A}^2 \text{ m}^2$). For each of the remaining 93 sub-regions
 170 (symmetrical across both hemispheres), PSDs of the constituent vertices were averaged to give a median PSD per Sub-region
 171 x Voice (Bottom and Top voices only) x Attend condition.

172 Next, the power at f_m (i.e. the ASSR power) during Attend and Unattend conditions was extracted separately for the
 173 Bottom and Top voices. The Attend versus Unattend ASSR power difference (Attend – Unattend) for each voice was
 174 computed as a percentage of the power at the Unattend condition (*% AU change*), representing a measure of the ASSR power
 175 enhancement due to selective attention. To obtain a visual estimation of the ASSR attentional enhancement across the cortical
 176 space, we mapped the *% AU change* over all sub-regions as shown in Figure 6. For a more concise numerical representation
 177 of the attentional contrast across the brain, the 93 sub-regions were subsequently categorized into 20 regions of interests
 178 (ROIs) per hemisphere according to the Brainnetome Atlas³⁹ (labels in Fig. 5). As before, the PSDs of all vertices within each
 179 ROI were median-averaged before extracting the power at f_m per Voice x Attend condition. The *% AU change* was computed
 180 and tabulated in Table 1, alongside the median *localizer power* per ROI.

181 2.5.5 Point spread function of a stimulated 41 Hz ASSR at the primary auditory cortex

182 We used the point spread function to characterize the spatial accuracy of the source localization method by illustrating the
 183 amount of signal spread occurring due to the source estimation of a single activated source, or in this case an area of activated
 184 sources. We computed the point spread function by first simulating a continuous 41 Hz sine wave at each vertex in the
 185 primary auditory cortex (see Figure 4B inset) for both hemispheres, followed by projecting the activity to the 306 MEG
 186 sensors, and finally projecting the estimated magnetic fields back to source space using the inverse solution that was obtained
 187 in the step above. This process was repeated for each participant using their individual noise covariance matrices and head
 188 geometries, then morphed to the fsaverage head template, and eventually averaged across all 27 participants to give the final
 189 solution illustrated in Figure 4B. The power of the simulated activity was fixed at $24.1 \cdot 10^{-26} \text{ A}^2 \text{ m}^2$, the group-averaged
 190 maximum power obtained in the MNE solution for the Middle voice localizer.

191 2.5.6 Cluster-based permutation of attentional modulation in areas outside the temporal cortex

192 To assess whether the attentional modulation is statistically driven by regions *outside* the temporal cortex, we adopted a
 193 cluster-based permutation test⁵⁹ using the PSD of each individual's MNE solution for the ASSR data (computed above in
 194 section 2.5.4): For each voice, a t-statistic was computed for every vertex using the difference between Attend and Unattend
 195 conditions. Clusters were defined as contiguous vertices across space with $t > 2.06$, and computed using a spatial resolution
 196 of 1284 vertices to ensure that the test remained sensitive despite minute spatial differences in activity between participants.
 197 The sum of t-values within each cluster (T_{sum}) was computed and compared against a distribution of the largest T_{sum} obtained
 198 from each of 1024 random permutations of the condition labels prior to clustering. The difference was defined as significant
 199 if there existed any clusters with a p-value below 0.05. To test if there was any region *outside* the temporal cortex that drives
 200 a statistically significant ASSR modulation, all vertices in the temporal cortex were excluded from clustering in the first a
 201 cluster-based permutation test. For comparison, we conducted a second cluster permutation test including all regions of the
 202 cortex.
 203
 204

3. Results

3.1 Behavioural results

Results from the MDT task showed that overall participants performed significantly above the chance level of 33% ($M = 67\%$, $SD = 21.7\%$; $t(29) = 8.30$, $p_{\text{one-tailed}} < 0.001$). As described above, under 2.1 Participants, two participants were excluded from further analyses to give a final sample size of 27 participants for subsequent MEG analyses. MDT task performance was not significantly different between directing attention to Bottom and Top voice ($p_{\text{two-tailed}} = 0.92$).

3.2 MEG results

3.2.1 Sensor space

We used sensor space analysis of MEG data to evaluate our primary hypothesis: Selective attention to frequency-tagged melody streams enhances the magnitude of the ASSR corresponding to the attended stream. To extract the effect of selective attention on the ASSR for each participant, we computed the average ASSR power spectrum across gradiometer sensors for all six conditions: Bottom-Attend, Bottom-Unattend, Top-Attend, Top-Unattend, Middle voice - Attend Bottom, Middle voice - Attend Top. For each of these conditions, we also calculated the average ERF sustained field to validate that our task successfully manipulated selective attention. Figure 2 shows the across subject grand average ASSR power spectra. The ASSR peaks for each voice can be observed clearly at the respective modulation frequencies of 39 (Bottom), 41 (Middle) and 43 (Top) Hz.

3.2.1.1 Attention and ASSR power

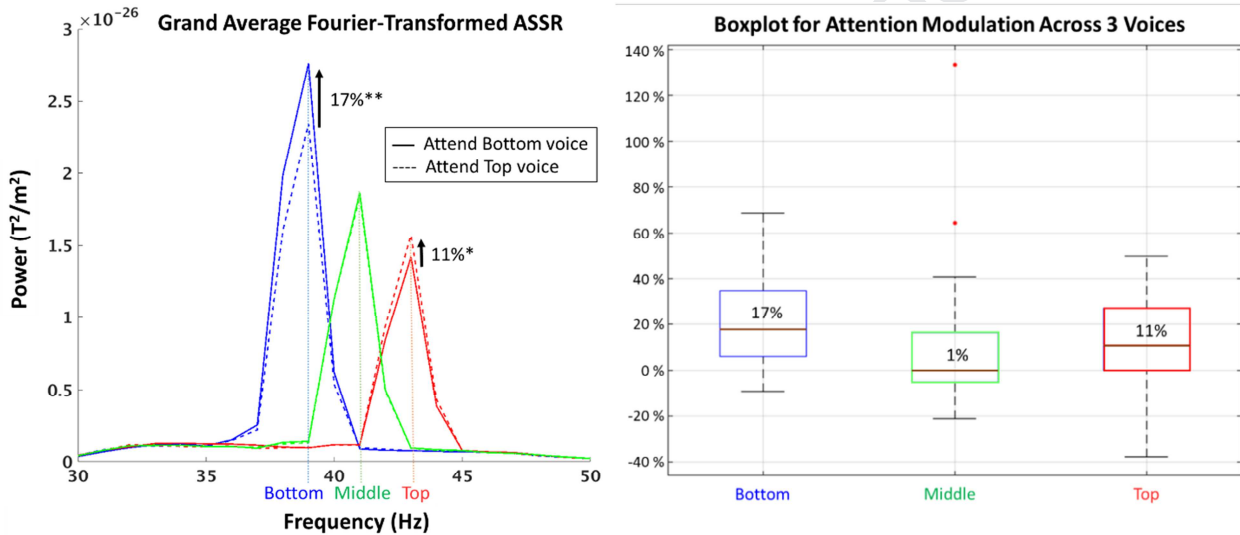


Figure 2. (Left panel) Across subject Grand Average ASSR power spectra for all conditions. ASSR power increased significantly when participants attended the corresponding Bottom (39 Hz - blue) or Top (43 Hz - red) voice. For the reference Middle voice (41 Hz - green), there was no significant difference between Attend Bottom and Attend Top. Arrows indicate median percentage attentional enhancement across all 27 participants. $p < 0.01^{**}$, $p < 0.05^{*}$

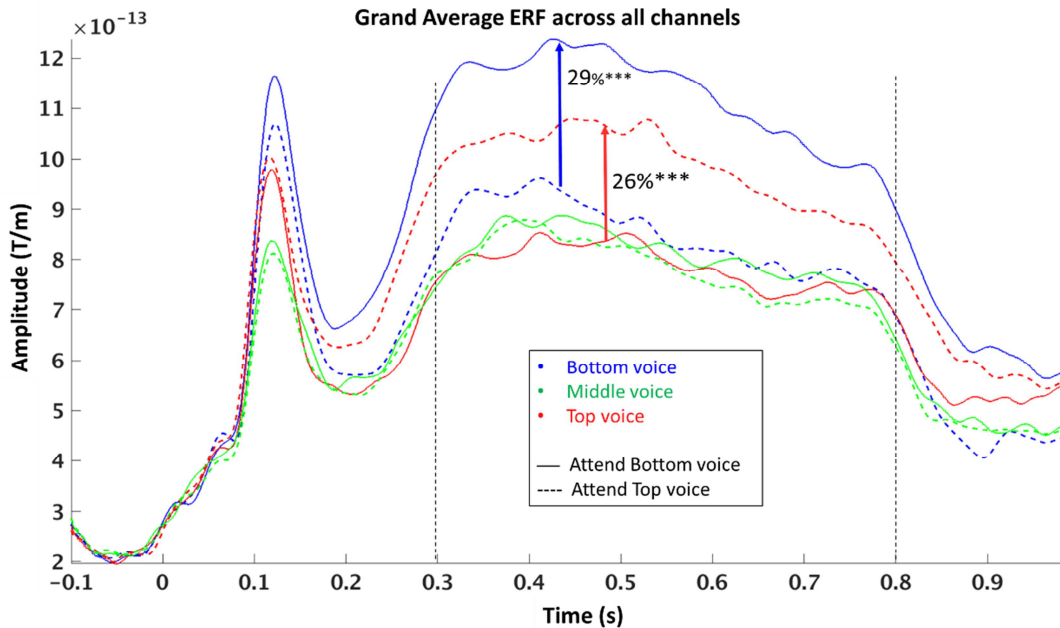
(Right panel) Boxplot showing the distribution of all 27 participant's percentage attentional change for the 3 voices. Median values are marked with brown lines and displayed in each box, while the bottom and top edges of each box indicated the 25 % and 75 % percentiles respectively. Outliers beyond the whiskers are plotted with red dots.

The Attend versus Unattend contrasts, using mean power (all units are in T^2/m^2) at f_m for the Bottom and Top voices, yield significant differences with a higher power for the Attend ($M_{\text{bottom}} = 2.80 \cdot 10^{-26}$, $SD_{\text{bottom}} = 3.3 \cdot 10^{-26}$; $M_{\text{top}} = 1.60 \cdot 10^{-26}$, $SD_{\text{top}} = 1.6 \cdot 10^{-26}$) compared to Unattend ($M_{\text{bottom}} = 2.39 \cdot 10^{-26}$, $SD_{\text{bottom}} = 2.7 \cdot 10^{-26}$; $M_{\text{top}} = 1.45 \cdot 10^{-26}$, $SD_{\text{top}} = 1.5 \cdot 10^{-26}$) condition ($t(27)_{\text{bottom}} = 3.51$, $p_{\text{two-tailed, bottom}} = 0.0016$; $t(27)_{\text{top}} = 2.62$, $p_{\text{two-tailed, top}} = 0.014$). These differences are expressed as a percentage of increase relative to the Unattend condition, and indicated with arrows in Figure 2 (left panel), alongside the spread of the data across individual participants (see Fig. 2, right panel). These results confirmed our primary hypothesis that selective attention enhances ASSR power, and at an average of 14 % across both Bottom and Top voices. There was no significant difference in ASSR enhancement between the Bottom and Top voice ($t(27) = 1.22$, $p_{\text{two-tailed}} = 0.24$). As expected, the ASSR enhancement was specific for the selectively attended voice, and was not observed on the Middle voice which participants were never instructed to attend to. Accordingly, there was no significant difference ($t(27) = 0.33$, $p_{\text{two-tailed}} = 0.74$) between Attend Bottom ($M = 1.90 \cdot 10^{-26}$, $SD = 2.0 \cdot 10^{-26}$) and Attend Top ($M = 1.89 \cdot 10^{-26}$, $SD = 2.1 \cdot 10^{-26}$) for the Middle voice.

3.2.1.2 Attention and ERFs

To validate that the MDT task manipulated attention successfully, we calculated the average ERF sustained field amplitude per Voice \times Attend condition. The results from contrasting the Attend versus Unattend ERF showed significant differences for the Bottom ($t(27) = 5.55$, $p_{\text{two-tailed}} < 0.001$) and Top ($t(27) = 6.27$, $p_{\text{two-tailed}} < 0.001$) voices. As with the ASSR,

246 for the non-attended Middle voice, there was no significant difference between Attend Bottom and Attend Top ($t(27) = 1.18$,
 247 $p_{\text{two-tailed}} = 0.25$). These ERF results serve as supporting evidence to show that selective attention was successfully
 248 manipulated as intended in this experiment (i.e directed exclusively to the instructed voice). The subject grand averaged ERFs
 249 per condition are illustrated in Figure 3 with arrows indicating the attentional enhancement [29 % (Bot); 26 % (Top)].



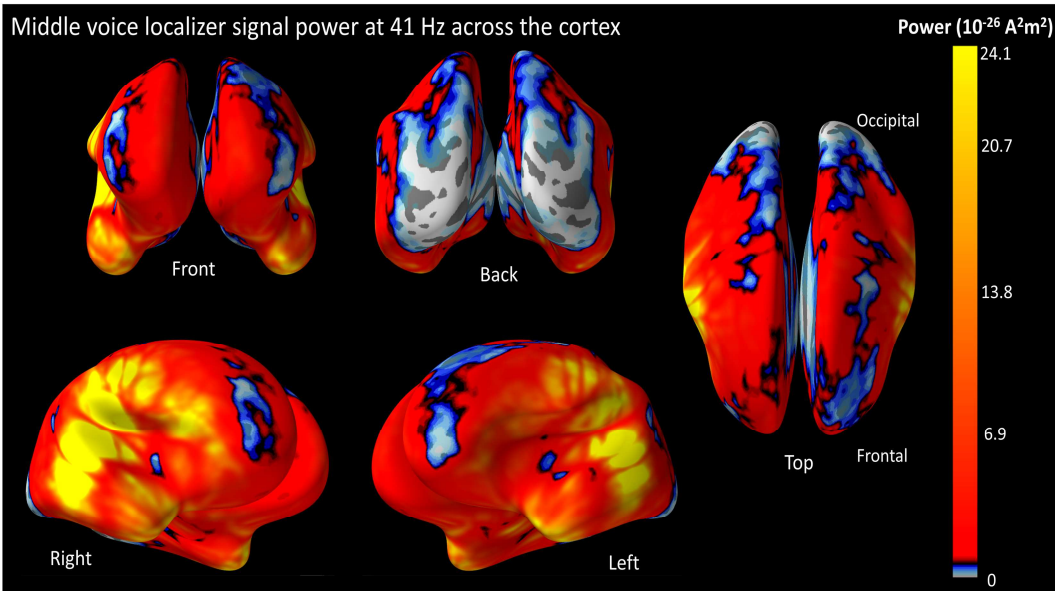
250
 251 **Figure 3.** Across subject Grand Average ERF for all conditions. The amplitude of the ERF sustained field was averaged across 300-800ms
 252 post-stimulus (black vertical dashed lines) and used for comparison between Attend versus Unattend conditions. As with the ASSR results,
 253 when participants attended the Bottom (blue) or Top (red) voice, corresponding ERF amplitudes increased significantly. There was no
 254 significant difference between Middle voice – Attend Bottom and Middle voice - Attend Top (green). Arrows indicate median percentage
 255 attentional enhancement across all 27 participants. $p < 0.001$ ***

256 3.2.2 Source space

257 Our secondary aim to determine the cortical distribution of neural sources that are involved in ASSR expression (section
 258 3.2.2.1 below) and their sensitivity to attentional modulation (section 3.2.2.2 below) was addressed with source space MEG
 259 analysis.

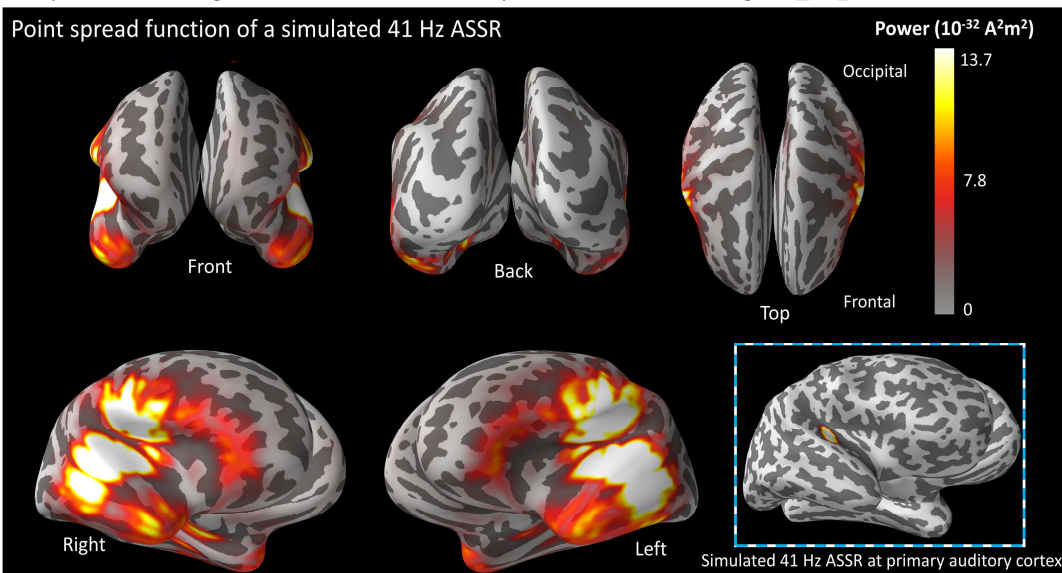
260 3.2.2.1 Location of ASSR Sources

261 To identify the cortical areas involved in ASSR expression, a distributed MNE source estimate of the Middle voice
 262 localizer power was computed, revealing multiple ASSR sources that originate mainly from the temporal, parietal and frontal
 263 cortices (Figure 4A). These source positions are coherent with the results of previous studies supporting ASSR activation
 264 sites extending beyond the auditory cortex⁴⁰⁻⁴². Unsurprisingly, sources with the strongest power were found in the primary
 265 auditory cortical regions, followed by parietal and frontal sources. In addition, the point spread function (see 2.5.5 above for
 266 details) for a simulated 41 Hz sine wave at the left and right auditory cortices was computed to assess whether the obtained
 267 ASSR sources were independent from one another or a result from a single signal in the primary auditory cortex spreading
 268 (Figure 4B). Notably, the modelled point spread function displayed a much lower maximum power at $13.7 \cdot 10^{-32} \text{ A}^2 \text{m}^2$,
 269 compared to the MNE solution with its maximum power at $24.1 \cdot 10^{-26} \text{ A}^2 \text{m}^2$, as well as less extensive coverage of the cortex.
 270 This shows that there exist large and systematic differences between the point spread model and our observed ASSR sources,
 271 and that the MNE source estimate cannot be explained solely by the signal spread of the primary auditory source.
 272



273
274
275
276
277
278

Figure 4A. ASSR power at 41 Hz for the Middle voice localizer across the cortex. The MNE solution for the Middle voice was used to estimate the location and strength of ASSR sources. Multiple ASSR sources were found over the entire cortical sheet with the strongest located in the primary auditory cortex. Other relatively strong sources were distributed over the temporal as well as parietal cortices, while sources with moderate activity were observed in the frontal region. Overall, the ASSR was stronger in the right than left hemisphere. The strength of the ASSR is described by the colour bar on the rightmost end.



279
280
281
282
283
284

Figure 4B. Point spread function of a simulated 41 Hz ASSR at the primary auditory cortex (both hemispheres). The power of the simulated ASSR sources (bottom-right inset) was adjusted to $24.1 \cdot 10^{-26} \text{ A}^2\text{m}^2$, the maximum power of the group-averaged Middle voice localizer. After applying the inverse solution, the resultant point spread function gave a lower group-averaged maximum power of $13.7 \cdot 10^{-32} \text{ A}^2\text{m}^2$.

285

3.2.2.2 Cluster-based permutation

286

When testing for attentional ASSR modulation *outside the temporal cortex* (thus excluding vertices in the temporal cortex), cluster-based permutation results revealed a significant ASSR attentional enhancement for the Bottom ($p_{\text{two-tailed}} = 0.002$) and Top ($p_{\text{two-tailed}} = 0.013$) voices, but not the non-attended Middle voice ($p_{\text{two-tailed}} = 0.71$). For the Bottom voice, the result was driven by clusters in the middle frontal gyrus, inferior frontal gyrus, orbital gyrus, inferior parietal lobule, postcentral gyrus and insular gyrus. For the Top voice, the result is driven by clusters in the precentral gyrus, inferior parietal lobule, postcentral gyrus and insular gyrus (see Fig. 5A).

292

Similarly, when testing for ASSR attentional modulation *across the entire cortex* (i.e. including the temporal cortex), the results showed a significant ASSR attentional enhancement for the Bottom ($p_{\text{two-tailed}} = 0.002$) and Top ($p_{\text{two-tailed}} = 0.013$) voices, but not the Middle voice ($p_{\text{two-tailed}} = 0.71$). As can be seen by comparing Figures 5A and 5B, the resultant ROIs are identical between these analyses, apart from additional vertices in the Superior Temporal Gyrus, Middle Temporal Gyrus and

295

296
297
298

Posterior Superior Temporal Sulcus that formed clusters in the latter test, contributing to the Bottom voice attentional enhancement (see Fig. 5B).

All Clusters With $p < 0.05$

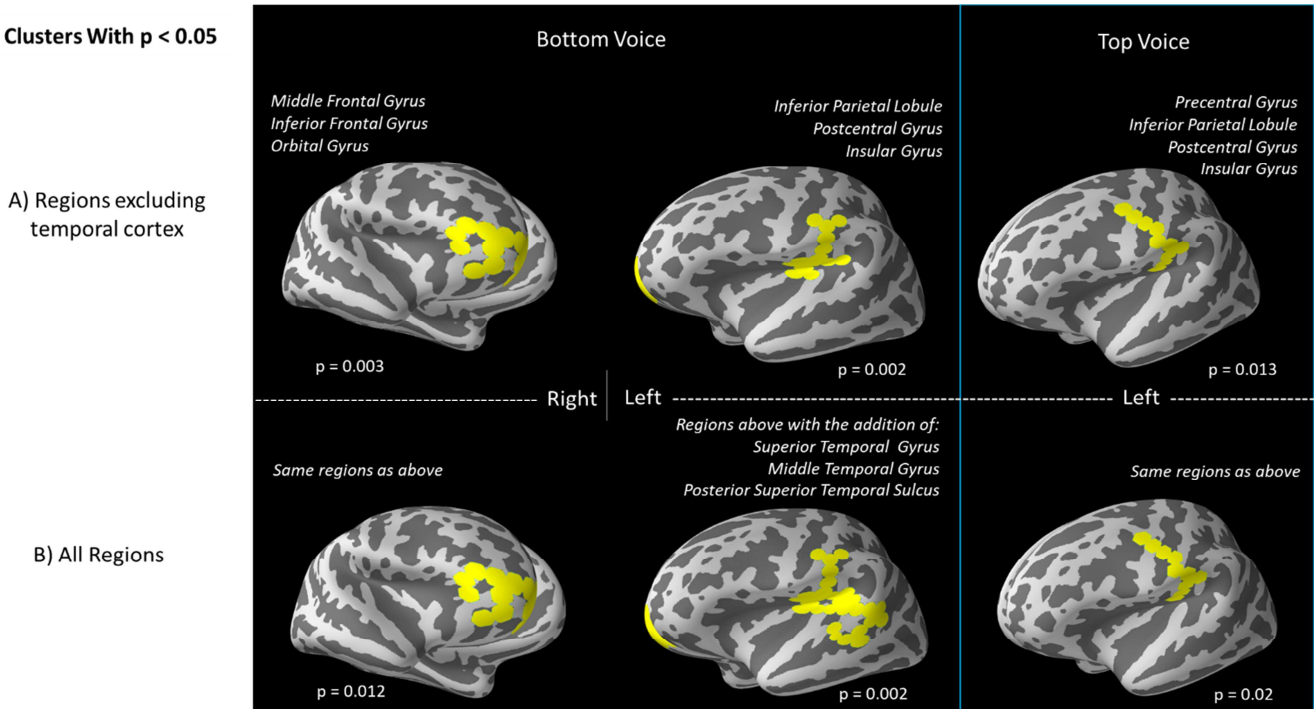
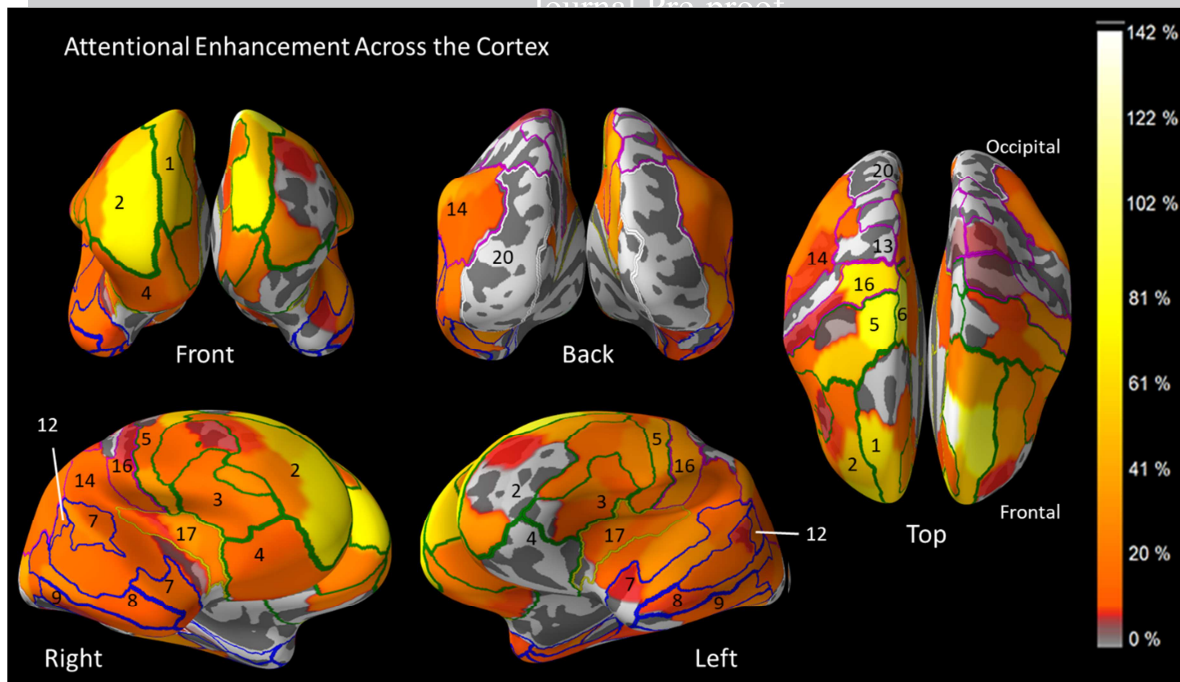
299
300
301
302
303
304
305
306

Figure 5. All clusters with $p < 0.05$ obtained from cluster-based permutation tests of the Attend-Unattend contrast for the Bottom (left) and Top (right) voices. The p-value of each cluster is displayed below the brain, while ROIs containing vertices that belong to the cluster are described in *italics* above the brain. A) Top row: Clusters obtained when vertices in the temporal cortex are excluded from clustering; B) Bottom row: Clusters obtained when vertices from all regions, including the temporal cortex, were allowed to form clusters. The ROIs are generally the same whether or not the temporal cortex is included during clustering, with the exception of the Bottom voice left hemispheric cluster which included three additional temporal ROIs as indicated.

3.2.2.3 Average ASSR Attentional Enhancement across the cortex

To evaluate how much each area involved in ASSR expression is modulated by selective attention, we computed the % *AU change* - a measure of the relative ASSR attentional enhancement - across 93 sub-regions per cortical hemisphere for the Bottom and Top voices. Figure 6 shows the voice-averaged % *AU change* across these sub-regions. The frontal cortex shows a wide range of attentional modulation effects, with some focal parts exhibiting very strong attentional ASSR enhancement above 80 % (yellow) while other areas display moderately strong attentional effect around 40 % (orange). In contrast, temporal and parietal regions display weaker but more homogeneous distribution of attentional modulation across sub-regions, with ASSR enhancements typically around 20 - 25 % (dark orange).

314



315
316 **Figure 6.** Distribution of ASSR attentional enhancement across the cortex. The average percentage increase in ASSR power between
317 Attend and Unattend conditions across the Bottom and Top voices was computed and scaled according to the colour bar on the right.
318 Generally speaking, frontal regions display a 2 – 4 times larger attentional enhancement than temporal and parietal regions. The frontal
319 cortex also shows a wider range of attentional modulation effects across sub-regions, with some focal parts exhibiting above 80 %
320 attentional ASSR enhancement (yellow) while other areas display comparatively weaker attentional effect of around 40 % (orange). On
321 the other hand, temporal and parietal regions show more homogeneity in the distribution of attentional enhancement that revolves
322 around 20 - 25 % (dark orange). The 93 sub-regions can be categorized into 20 ROI labels per hemisphere as demarcated above. ROIs
323 in the frontal (green), temporal (blue), parietal (magenta), occipital (white) and insular/limbic (yellow) lobes are numbered according to the
324 Label # column in Table 1. Labels 10, 11, 15, 18 and 19 are located in the medial region between both hemispheres and thus not visible in
325 this figure.

326 Subsequently, we categorized the sub-regions into 20 ROIs per hemisphere and compiled the % AU change for each in Table
327 1, sorted in order of decreasing median localizer power across both hemispheres (BH column). Asterisks * mark the ROIs and
328 corresponding hemisphere containing vertices which belong to any cluster with $p < 0.05$ that drives the attentional effect, as
329 reported in the cluster-based permutation test above (section 3.2.2.2). The attention effect was distributed across all ROIs at
330 an average of ~ 15 %. ROIs in the frontal gyrus appear to be most strongly and consistently enhanced by attention, with the
331 left superior frontal gyrus (Label #1 in Tab. 1 and Fig. 5) showing up to 54 % attentional enhancement. Regions in the
332 temporal and parietal lobes displayed up to 27 % and 35 % attentional enhancement respectively. It is useful to note that while
333 some ROIs in the bottom rows of Table 1 have high % AU change (e.g. Lateral Occipital Cortex) that may suggest strong
334 attentional enhancement, localizer ASSR power in these areas were extremely weak (within the lowest 5 % of all sub-regions
335 for the Lateral Occipital Cortex). This calls for caution when interpreting whether the attentional enhancement in these
336 regions stems from the presence of true ASSR sources, or is likely a spurious result from noise or field spread.

Lobe	Label #	Regions of interest	Localizer Power ($A^2 m^2$)			% AU Change	
			BH	LH	RH	LH	RH
Temporal	7	Superior temporal gyrus	1.74E-25	1.24E-25	2.25E-25	19%*	15%
Temporal	8	Middle temporal gyrus	1.29E-25	1.14E-25	1.43E-25	18%*	11%
Temporal	12	Posterior superior temporal sulcus	1.27E-25	1.06E-25	1.48E-25	13%*	14%
Frontal	3	Inferior frontal gyrus	8.36E-26	6.42E-26	1.03E-25	15%	18%*
Temporal	9	Inferior temporal gyrus	5.33E-26	5.87E-26	4.79E-26	13%	14%
Parietal	16	Postcentral gyrus	4.79E-26	3.84E-26	5.74E-26	17%*	11%*
Insular	17	Insular gyrus	3.77E-26	2.23E-26	5.32E-26	14%*	15%*
Frontal	5	Precentral gyrus	3.50E-26	2.79E-26	4.21E-26	15%	25%*
Temporal	10	Fusiform gyrus	3.09E-26	2.72E-26	3.46E-26	27%	9%
Temporal	11	Parahippocampal gyrus	2.96E-26	2.74E-26	3.17E-26	-14%	10%
Frontal	4	Orbital gyrus	2.87E-26	2.53E-26	3.21E-26	-8%	15%*
Parietal	14	Inferior parietal lobule	1.61E-26	9.93E-27	2.23E-26	13%*	14%*
Frontal	6	Paracentral lobule	1.40E-26	1.52E-26	1.28E-26	-5%	59%

Frontal	2	Middle frontal gyrus	1.15E-26	8.79E-27	1.41E-26	18%	25%*
Parietal	15	Precuneus	1.02E-26	1.12E-26	9.25E-27	-3%	35%
Frontal	1	Superior frontal gyrus	8.96E-27	6.67E-27	1.13E-26	54%	32%
Occipital	20	Lateral occipital cortex	8.18E-27	8.01E-27	8.35E-27	20%	36%
Parietal	13	Superior parietal lobule	8.12E-27	6.74E-27	9.49E-27	-6%	0%
Occipital	19	MedioVentral occipital cortex	6.4448E-27	6.23E-27	6.74E-27	9%	20%
Limbic	18	Cingulate gyrus	6.20E-27	5.12E-27	7.28E-27	12%	14%

Table 1. % AU change for 20 ROIs, sorted in order of decreasing bi-hemispheric localizer power (BH column). The localizer power and % AU change are shown for the Left Hemisphere (LH), Right Hemisphere (RH) and Both Hemisphere average (BH). The first column names the lobe in which the ROI belongs, while the Label # column indicates its position numbered in Figure 6 above. Coloured rows highlight ROIs belonging to the temporal (blue), frontal (green), parietal (pink), occipital (white) and insular/limbic (yellow) lobes. Asterisks * indicate that the ROI contains vertices belonging to clusters driving the significant effect in the cluster-based permutation test.

4. Discussion

This study was conducted with the primary aim of examining whether selective attention to frequency-tagged melody streams (in this study coined *voices*) that are presented diotically enhances the magnitude of the ASSR specifically to the selectively attended voice. Consistent with our primary hypothesis, we observed significant enhancement of ASSR power due to selective attention in MEG sensor space (see Fig. 2 and 3).

As a secondary aim, we also examined the cortical distribution of neural sources that are involved in ASSR expression and their sensitivity to attentional modulation. To this aim, we analysed the MEG data using an MNE distributed source model, and found significant ASSR enhancement outside the temporal cortices driven by clusters in the frontal and parietal regions (see Fig. 5). We then mapped out the across-subject grand average ASSR attentional enhancement over the cortical sheet and observed differences in the degree of attentional enhancement across frontal, temporal and parietal ROIs (see Fig. 6 and Table 1). While some previous studies have reported ASSR modulation when shifting selective attention between sensory modalities¹²⁻¹⁴ and between ears (as in dichotic listening experiments)^{6, 15-17}, our study investigates this effect on diotically presented sound streams that can only be distinguished by their perceptual content (i.e. pitch and timing). This is important as content-based separation is an important part of selective auditory attention in central to functions such as speech recognition and music listening. The following section discusses the key findings and relevance of the current study.

4.1 Attentional enhancement of ASSR

Overall, our results showed that selective attention enhanced the 40 Hz ASSR power by an average of 14 % (see Fig. 2 and 3). We also demonstrated that this enhancement was specific to the attended Bottom and Top voices, but did not spread to the adjacent non-attended Middle voice, both in sensor space and in source space. To the best of our knowledge, this is the first time any study has reported clear findings of ASSR attentional enhancement based solely on perceptual separation of stimuli sound content. While our results revealed stronger attentional modulation for the Bottom voice ASSR than the Top voice ASSR, we also noted that the mean Bottom voice ASSR power was higher than that of the Top voice, regardless of attentional condition. We believe that the main reason behind a lower Top voice ASSR power is that its volume was reduced to -10 dB relative to the Bottom Voice (as described under Methods). The loudness of the voices was adjusted to be subjectively equal for the MDT task, in order to compensate for the subjective amplification of higher pitch sounds in human hearing³², and this has created general ASSR power differences between the voices⁸. This volume difference as well as other differences between the voices, such as that in carrier frequency and modulation frequency, might also have contributed to the observed attentional differences across the Bottom and Top voices, although additional studies are required to further investigate this. The modulation in ASSR power due to selective attention supports the notion of a top-down regulated gain control mechanism of attention, proposed by many authors in the past^{7, 20-23}. Importantly, the results provide the first clear evidence that selective attention enhances the neuronal representation of an attended sound stream, even when the attended stream is not spatially separated from other sounds, as in dichotic listening designs.

4.2 Location of the ASSR and its Attentional Enhancement:

Regarding the cortical distribution of ASSR sources and their sensitivity to attentional modulation, MNE results revealed ASSR sources originating from a variety of frontal, temporal and parietal regions (Fig. 4A). The accompanying point spread function (Fig. 4B) of the primary auditory cortex can be used to gauge whether these sources are truly active and independent or caused by field spread from strong sources within the primary auditory cortex. Taken together, the systematic differences between the point spread model and the observed ASSR source model favours an interpretation where frontal sources are independently active from the primary auditory sources. Although several activated regions in the parietal and secondary auditory cortices overlap with the point spread function, the much larger power generated by the MNE solution indicates that additional sources outside the primary auditory cortex must be present to contribute to the additional signal power. As further support for this interpretation, previous EEG⁴² and positron emission tomography (PET)⁴⁰⁻⁴¹ studies have also found multiple sources generating the 40 Hz ASSR, including many regions outside the auditory pathway. These regions, especially the frontal areas, are commonly overlooked in ASSR-attention studies, which typically place exclusive focus on stronger sources

386 within the primary auditory cortex¹²⁻¹⁷, especially when the ASSR source is modelled as dipoles. To the best of our
387 knowledge, no present study has reported any attentional effect on sources outside the temporal cortex, thus highlighting the
388 novelty of our results demonstrating a significant attentional enhancement from these sources.

389 Complementary to these results, the subject-averaged degree of attentional enhancement was mapped over the entire
390 cortical sheet to provide a visual understanding of the ASSR attentional distribution. However, as a rule of caution, we
391 recommend readers to also consider the ASSR source activity (Fig. 4A/B) of an area when evaluating whether that area
392 directly expresses an ASSR and an associated attentional modulation, or whether the observed enhancement is an indirect
393 artefact of field spread from nearby strong sources. For example, no obvious independent ASSR sources were found in the
394 Middle Temporal Gyrus (Label #8) and Inferior Temporal Gyrus (Label #9), suggesting that the observed ASSR and
395 attentional enhancement at these areas are likely due to field spread from adjacent regions. Conversely, judging from Figure
396 4, the Superior Temporal Gyrus (Label #7) and Postcentral Gyrus (Label #16) both contain strongly activated and visibly
397 independent ASSR sources, thus providing more convincing evidence that substantiates the presence of actual ASSR
398 enhancement. This is further supported by the fact that these ROIs contain vertices that belong to clusters driving the
399 significant attentional effect. Interestingly, our source level analysis seems to suggest that there are large differences in the
400 degree of attentional modulation across anatomical regions, with high levels of modulation outside the auditory system.
401 Indeed, we found that the ASSR localized to the frontal gyrus displayed the largest average degree of attentional modulation.
402 As seen in Figure 6, most cortical areas display a ~ 25 % average attentional enhancement from selective attention, whereas
403 regions in the prefrontal cortex showed up to 60 - 80 % enhancement, with a local concentration in the middle frontal gyrus.
404 This is not surprising per se as the prefrontal cortex has been long regarded as the centre of attentional control in neuroscience
405 literature involving auditory attention^{29-30, 50-51} as well as attention in other sensory modalities²⁷⁻²⁸. In addition to the frontal
406 cortices, we also found relatively more homogeneous average attentional enhancement across the temporal and parietal
407 regions of ~ 25 %. Similar to our findings, attentional enhancement of the ASSR in the auditory cortex has been reported by
408 several studies, although limited to spatial^{6, 15-17} and intermodal¹²⁻¹⁴ attention. Evidence of auditory attentional modulation in
409 the parietal cortex has also been reported in previous studies^{29, 52-55}, although not within the ASSR domain, owing perhaps to
410 the lack of documentation on ASSR sources outside the auditory cortex. In relation to this, the motor cortex, housed by the
411 parts of the frontal and parietal lobes, is known to exhibit a robust entrainment to sensory stimulation rhythms that is also
412 enhanced from attention^{53, 56-58}. Since the ASSR may be conceptualized as an entrainment (to the stimulus) itself, it is
413 reasonable that ASSR activity and its attentional modulation was found in the motor cortex.

414 4.3 Overcoming challenges in ASSR attentional modulation research

415 Since the current literature is inconsistent about whether and how intramodal auditory selective attention modulates the
416 ASSR, a consensus on this topic has yet not been reached. This is likely attributed to factors related to stimuli, task and
417 analytical differences. For instance, *first*, using competing stimuli with too similar properties can lead to weak perceptual
418 separation and subsequently less effective selective attention. In many cases, the competing stimuli have similar or even
419 identical carrier frequencies^{15-16, 46}, and simultaneous onsets⁴⁷, making it difficult for participants to differentiate between
420 stimuli, thereby translating into a smaller ASSR power difference between Attend and Unattend conditions which the
421 measurement instrument and analysis approach may not be sensitive enough to pick up. *Second*, several studies adopted a
422 target detection task, placing salient targets, such as a change in frequency or intensity, in both the attended stream and
423 distractor streams^{16-17, 47}. This can result in a bottom-up effect from the distractor during the appearance of targets, thereby
424 reducing the degree of selective attention to the attended stream. Moreover, there is evidence demonstrating that salient
425 events amplify the ASSR in the unattended stream⁴⁸, which can also reduce the Attend vs Unattend ASSR contrast. A *third*
426 reason could be the narrow focus on temporal auditory core regions in source models used to localize the ASSR by most
427 studies^{15-16, 47}. Although the ASSR is strongest at these areas, a one-sided focus on these regions risks overlooking other areas
428 such as the frontal and parietal cortices that can exhibit greater selective attention effects, as is indeed seen in our current
429 study. In this study, we sought to alleviate these potential pitfalls by improving stream separability with the use of tones that
430 are easily separable by timing as well as pitch, inspecting the corresponding ERFs to check for successful manipulation of
431 selective attention, adopting a melody tracking task in place of target detection, and using a distributed source model to
432 examine the entire cortical sheet for ASSR activity.

433 4.4 Limitations of current study:

434 While we believe that our present results make novel contributions to the existing literature on ASSR methodology as well
435 as to the neuroscientific understanding of selective auditory attention, the study has several limitations and calls for further
436 work to clarify the present results. Primarily speaking, our results build on ASSR sources generated by AM frequencies close
437 to 40 Hz and may not be generalizable across ASSRs at other frequencies as they tend to display different source distribution
438 patterns⁴². Secondly, while the use of sine tones that are separated in time may not be an accurate representation of natural
439 auditory mixtures such as a large choir or a symphony orchestra, the ASSR approach developed in this study is the first of its
440 kind and serves as a stepping stone for future studies on selective attention in more natural and complex environments.
441 Thirdly, while the sensor-space and source-space analysis provides statistical evidence affirming the attentional modulation
442 of the ASSR (primary aim) per se, the current approach can demarcate cortical contributions to ASSR modulation broadly
443 (i.e. attentional effect likely in the frontal-parietal cortices), but cannot conclusively pin-point the specific locations

444 (especially at a vertex level) that are susceptible to ASSR attentional modulation. In addition, it is difficult to discern whether
445 a specific region exhibits true attention effects or is instead a result of point-spread from nearby sources, and this is currently
446 dependent to some extent, on subjective interpretation of the reported findings. Nonetheless, this study can serve as a
447 guideline to form region-specific, a-priori hypotheses, for more confirmative investigations in the future.

448 *4.5 Conclusions*

449 In this study, we demonstrated that selective attention strongly enhances the ASSR, and that this effect can be robustly
450 observed at sensor as well as source level analysis of MEG data. At source level, across-subject averages suggest that ASSR
451 attention enhancement vary widely across the cortex, and is strongest in the frontal regions, which is well-aligned with
452 current literature marking the pre-frontal cortex as the centre for attentional control^{27-28, 30}. Notably, this work highlights the
453 importance of including non-auditory areas in ASSR application studies and advocates a novel 'beyond the temporal cortex'
454 perspective on ASSR modulation. Overall, the current study presents clear evidence that selective auditory attention to the
455 sound content of musical streams increases the ASSR power of the attended stream in temporal, frontal and parietal cortical
456 regions. Since the ASSR can readily capture these attentional changes in a stimuli-precise manner, it can serve as a useful
457 tool for future research on selective attention in complex auditory scenarios.

458 **Conflicts of Interests**

459 None

460 **Acknowledgments**

461 Data for this study was collected at NatMEG, the National Facility for Magnetoencephalography (<http://natmeg.se>),
462 Karolinska Institutet, Sweden. The NatMEG facility is supported by Knut and Alice Wallenberg Foundation
463 (KAW2011.0207). This study was supported by the Swedish Foundation for Strategic Research (SBE 13-0115).

- 465 1. Cherry, E. C., Some Experiments on the Recognition of Speech, with One and with Two Ears. *The Journal of the*
466 *Acoustical Society of America* **1953**, 25 (5), 975-979.
- 467 2. Parbery-Clark, A.; Skoe, E.; Lam, C.; Kraus, N., Musician enhancement for speech-in-noise. *Ear and hearing* **2009**,
468 30 (6), 653.
- 469 3. Parbery-Clark, A.; Skoe, E.; Kraus, N., Musical Experience Limits the Degradative Effects of Background Noise on
470 the Neural Processing of Sound. *The Journal of Neuroscience* **2009**, 29 (45), 14100-14107.
- 471 4. Hansen, J. C.; Dickstein, P. W.; Berka, C.; Hillyard, S. A., Event-related potentials during selective attention to
472 speech sounds. *Biological Psychology* **1983**, 16 (3-4), 211-224.
- 473 5. Woods, D. L.; Hillyard, S. A.; Hansen, J. C., Event-related brain potentials reveal similar attentional mechanisms
474 during selective listening and shadowing. *Journal of Experimental Psychology: Human Perception and Performance* **1984**,
475 10 (6), 761-777.
- 476 6. Bidet-Caulet, A.; Fischer, C.; Besle, J.; Aguera, P.-E.; Giard, M.-H.; Bertrand, O., Effects of Selective Attention on
477 the Electrophysiological Representation of Concurrent Sounds in the Human Auditory Cortex. *The Journal of Neuroscience*
478 **2007**, 27 (35), 9252-9261.
- 479 7. Woldorff, M. G.; Gallen, C. C.; Hampson, S. A.; Hillyard, S. A.; Pantev, C.; Sobel, D.; Bloom, F. E., Modulation of
480 early sensory processing in human auditory cortex during auditory selective attention. *Proceedings of the National Academy*
481 *of Sciences of the United States of America* **1993**, 90 (18), 8722-8726.
- 482 8. Ross, B.; Borgmann, C.; Draganova, R.; Roberts, L. E.; Pantev, C., A high-precision magnetoencephalographic
483 study of human auditory steady-state responses to amplitude-modulated tones. *J Acoust Soc Am* **2000**, 108 (2), 679-91.
- 484 9. Regan, D., Human brain electrophysiology : evoked potentials and evoked magnetic fields in science and medicine.
485 Elsevier: New York, 1989.
- 486 10. Picton, T. W.; John, M. S.; Dimitrijevic, A.; Purcell, D., Human auditory steady-state responses. *Int J Audiol* **2003**,
487 42 (4), 177-219.
- 488 11. Lins, O. G.; Picton, T. W., Auditory steady-state responses to multiple simultaneous stimuli. *Electroencephalogr*
489 *Clin Neurophysiol* **1995**, 96 (5), 420-32.
- 490 12. Gander, P. E.; Bosnyak, D. J.; Roberts, L. E., Evidence for modality-specific but not frequency-specific modulation
491 of human primary auditory cortex by attention. *Hearing Research* **2010**, 268 (1), 213-226.
- 492 13. Saupe, K.; Schröger, E.; Andersen, S. K.; Müller, M. M., Neural Mechanisms of Intermodal Sustained Selective
493 Attention with Concurrently Presented Auditory and Visual Stimuli. *Frontiers in Human Neuroscience* **2009**, 3, 58.
- 494 14. Keitel, C.; Schröger, E.; Saupe, K.; Müller, M. M., Sustained selective intermodal attention modulates processing of
495 language-like stimuli. *Experimental Brain Research* **2011**, 213 (2), 321-327.
- 496 15. Müller, N.; Schlee, W.; Hartmann, T.; Lorenz, I.; Weisz, N., Top-Down Modulation of the Auditory Steady-State
497 Response in a Task-Switch Paradigm. *Frontiers in Human Neuroscience* **2009**, 3, 1.
- 498 16. Bharadwaj, H.; Lee, A. K. C.; Shinn-Cunningham, B., Measuring auditory selective attention using frequency
499 tagging. *Frontiers in Integrative Neuroscience* **2014**, 8 (6).
- 500 17. Lazzouni, L.; Ross, B.; Voss, P.; Lepore, F., Neuromagnetic auditory steady-state responses to amplitude modulated
501 sounds following dichotic or monaural presentation. *Clinical Neurophysiology* **2010**, 121 (2), 200-207.
- 502 18. Bharadwaj, H. M.; Lee, A. K. C.; Shinn-Cunningham, B. G., Measuring auditory selective attention using frequency
503 tagging. *Frontiers in Integrative Neuroscience* **2014**, 8, 6.
- 504 19. Cohen, D., Magnetoencephalography: detection of the brain's electrical activity with a superconducting
505 magnetometer. *Science* **1972**, 175 (4022), 664-6.
- 506 20. Hillyard, S. A.; Vogel, E. K.; Luck, S. J., Sensory gain control (amplification) as a mechanism of selective attention:
507 electrophysiological and neuroimaging evidence. *Philosophical transactions of the Royal Society of London. Series B,*
508 *Biological sciences* **1998**, 353 (1373), 1257-70.
- 509 21. Hillyard, S. A.; Hink, R. F.; Schwent, V. L.; Picton, T. W., Electrical Signs of Selective Attention in the Human
510 Brain. *Science* **1973**, 182 (4108), 177-180.
- 511 22. Kerlin, J. R.; Shahin, A. J.; Miller, L. M., Attentional Gain Control of Ongoing Cortical Speech Representations in a
512 "Cocktail Party". *The Journal of Neuroscience* **2010**, 30 (2), 620-628.
- 513 23. Lee, A. K. C.; Larson, E.; Maddox, R. K.; Shinn-Cunningham, B. G., Using neuroimaging to understand the cortical
514 mechanisms of auditory selective attention. *Hearing Research* **2014**, 307, 111-120.
- 515 24. Schoonhoven, R.; Boden, C. J. R.; Verbunt, J. P. A.; de Munck, J. C., A whole head MEG study of the amplitude-
516 modulation-following response: phase coherence, group delay and dipole source analysis. *Clinical Neurophysiology* **2003**,
517 114 (11), 2096-2106.
- 518 25. Steinmann, I.; Gutschalk, A., Potential fMRI correlates of 40-Hz phase locking in primary auditory cortex, thalamus
519 and midbrain. *NeuroImage* **2011**, 54 (1), 495-504.
- 520 26. Lamminmäki, S.; Parkkonen, L.; Hari, R., Human Neuromagnetic Steady-State Responses to Amplitude-Modulated
521 Tones, Speech, and Music. *Ear and Hearing* **2014**, 35 (4), 461-467.
- 522 27. Cohen, R. A., Attention and the Frontal Cortex. In *The Neuropsychology of Attention*, Springer US: Boston, MA,
523 2014; pp 335-379.
- 524 28. Foster, J. K.; Eskes, G. A.; Stuss, D. T., The cognitive neuropsychology of attention: A frontal lobe perspective.
525 *Cognitive Neuropsychology* **1994**, 11 (2), 133-147.

- 526 29. Shomstein, S.; Yantis, S., Parietal Cortex Mediates Voluntary Control of Spatial and Nonspatial Auditory Attention. *The Journal of Neuroscience* **2006**, *26* (2), 435-439.
- 527
- 528 30. Plakke, B.; Romanski, L. M., Auditory connections and functions of prefrontal cortex. *Frontiers in neuroscience*
- 529 **2014**, *8*, 199-199.
- 530 31. Akerstedt, T.; Gillberg, M., Subjective and objective sleepiness in the active individual. *The International journal of*
- 531 *neuroscience* **1990**, *52* (1-2), 29-37.
- 532 32. Robinson, D. W.; Dadson, R. S., A re-determination of the equal-loudness relations for pure tones. *British Journal of*
- 533 *Applied Physics* **1956**, *7* (5), 166.
- 534 33. Taulu, S.; Kajola, M.; Simola, J., Suppression of Interference and Artefacts by the Signal Space Separation Method.
- 535 2004; Vol. 16, p 269-75.
- 536 34. Taulu, S.; Simola, J., Spatiotemporal signal space separation method for rejecting nearby interference in MEG
- 537 measurements. *Physics in medicine and biology* **2006**, *51* (7), 1759-68.
- 538 35. Oostenveld, R.; Fries, P.; Maris, E.; Schoffelen, J.-M., FieldTrip: Open Source Software for Advanced Analysis of
- 539 MEG, EEG, and Invasive Electrophysiological Data. *Computational Intelligence and Neuroscience* **2011**, *2011*, 9.
- 540 36. Gramfort, A.; Luessi, M.; Larson, E.; Engemann, D.; Strohmeier, D.; Brodbeck, C.; Goj, R.; Jas, M.; Brooks, T.;
- 541 Parkkonen, L.; Hämäläinen, M., MEG and EEG data analysis with MNE-Python. *Frontiers in Neuroscience* **2013**, *7* (267).
- 542 37. Fischl, B., FreeSurfer. *Neuroimage* **2012**, *62* (2), 774-81.
- 543 38. Picton, T. W.; Woods, D. L.; Proulx, G. B., Human auditory sustained potentials. I. The nature of the response.
- 544 *Electroencephalography and clinical neurophysiology* **1978**, *45* (2), 186-197.
- 545 39. Fan, L.; Chu, C.; Li, H.; Chen, L.; Xie, S.; Zhang, Y.; Yang, Z.; Jiang, T.; Laird, A. R.; Wang, J.; Zhuo, J.; Yu, C.;
- 546 Fox, P. T.; Eickhoff, S. B., The Human Brainnetome Atlas: A New Brain Atlas Based on Connectional Architecture.
- 547 *Cerebral Cortex* **2016**, *26* (8), 3508-3526.
- 548 40. Reyes, S. A.; Lockwood, A. H.; Salvi, R. J.; Coad, M. L.; Wack, D. S.; Burkard, R. F., Mapping the 40-Hz auditory
- 549 steady-state response using current density reconstructions. *Hearing Research* **2005**, *204* (1), 1-15.
- 550 41. Reyes, S. A.; Salvi, R. J.; Burkard, R. F.; Coad, M. L.; Wack, D. S.; Galantowicz, P. J.; Lockwood, A. H., PET
- 551 imaging of the 40 Hz auditory steady state response. *Hearing Research* **2004**, *194* (1), 73-80.
- 552 42. Farahani, E. D.; Goossens, T.; Wouters, J.; van Wieringen, A., Spatiotemporal reconstruction of auditory steady-
- 553 state responses to acoustic amplitude modulations: Potential sources beyond the auditory pathway. *NeuroImage* **2017**, *148*,
- 554 240-253.
- 555 43. Ross, B.; Herdman, A. T.; Pantev, C., Right Hemispheric Laterality of Human 40 Hz Auditory Steady-state
- 556 Responses. *Cerebral Cortex* **2005**, *15* (12), 2029-2039.
- 557 44. Schneider, P.; Scherg, M.; Dosch, H. G.; Specht, H. J.; Gutschalk, A.; Rupp, A., Morphology of Heschl's gyrus
- 558 reflects enhanced activation in the auditory cortex of musicians. *Nat Neurosci* **2002**, *5* (7), 688-694.
- 559 45. Weisz, N.; Lithari, C., Amplitude modulation rate dependent topographic organization of the auditory steady-state
- 560 response in human auditory cortex. *Hearing Research* **2017**, *354*, 102-108.
- 561 46. Mahajan, Y.; Davis, C.; Kim, J., Attentional Modulation of Auditory Steady-State Responses. *PLoS ONE* **2014**, *9*
- 562 (10), e110902.
- 563 47. Gander, P. E.; Bosnyak, D. J.; Roberts, L. E., Evidence for modality-specific but not frequency-specific modulation
- 564 of human primary auditory cortex by attention. *Hearing Research* **2010**, *268* (1), 213-226.
- 565 48. Shuai, L.; Elhilali, M., Task-dependent neural representations of salient events in dynamic auditory scenes.
- 566 *Frontiers in Neuroscience* **2014**, *8* (203).
- 567 49. Xiang, J.; Simon, J.; Elhilali, M., Competing Streams at the Cocktail Party: Exploring the Mechanisms of Attention
- 568 and Temporal Integration. *The Journal of Neuroscience* **2010**, *30* (36), 12084-12093.
- 569 50. Pugh, K. R.; Shaywitz, B. A.; Shaywitz, S. E.; Fulbright, R. K.; Byrd, D.; Skudlarski, P.; Shankweiler, D. P.; Katz,
- 570 L.; Constable, R. T.; Fletcher, J.; Lacadie, C.; Marchione, K.; Gore, J. C., Auditory Selective Attention: An fMRI
- 571 Investigation. *NeuroImage* **1996**, *4* (3), 159-173.
- 572 51. Tzourio, N.; El Massioui, F.; Crivello, F.; Joliot, M.; Renault, B.; Mazoyer, B., Functional Anatomy of Human
- 573 Auditory Attention Studied with PET. *NeuroImage* **1997**, *5* (1), 63-77.
- 574 52. Wu, C. T.; Weissman, D. H.; Roberts, K. C.; Woldorff, M. G., The neural circuitry underlying the executive control
- 575 of auditory spatial attention. *Brain Res* **2007**, *1134* (1), 187-98.
- 576 53. Besle, J.; Schevon, C. A.; Mehta, A. D.; Lakatos, P.; Goodman, R. R.; McKhann, G. M.; Emerson, R. G.; Schroeder,
- 577 C. E., Tuning of the Human Neocortex to the Temporal Dynamics of Attended Events. *The Journal of Neuroscience* **2011**, *31*
- 578 (9), 3176-3185.
- 579 54. Alain, C.; Arnott, S. R.; Hevenor, S.; Graham, S.; Grady, C. L., "What" and "where" in the human auditory system.
- 580 *Proceedings of the National Academy of Sciences* **2001**, *98* (21), 12301-12306.
- 581 55. Hill, K. T.; Miller, L. M., Auditory Attentional Control and Selection during Cocktail Party Listening. *Cerebral*
- 582 *Cortex* (New York, NY) **2010**, *20* (3), 583-590.
- 583 56. Horton, C.; D'Zmura, M.; Srinivasan, R., Suppression of competing speech through entrainment of cortical
- 584 oscillations. *Journal of neurophysiology* **2013**, *109* (12), 3082-3093.
- 585 57. Fujioka, T.; Ross, B.; Trainor, L. J., Beta-Band Oscillations Represent Auditory Beat and Its Metrical Hierarchy in
- 586 Perception and Imagery. *The Journal of Neuroscience* **2015**, *35* (45), 15187-15198.

- 587 58. Sameiro-Barbosa, C. M.; Geiser, E., Sensory Entrainment Mechanisms in Auditory Perception: Neural
588 Synchronization Cortico-Striatal Activation. *Frontiers in Neuroscience* 2016, 10 (361).
- 589 59. Maris, E.; Oostenveld, R., Nonparametric statistical testing of EEG- and MEG-data. *Journal of Neuroscience*
590 *Methods* **2007**, 164 (1), 177-190.
- 591

Journal Pre-proof

592 **Supplementary Information**593 *S1 Hemispheric lateralization of the ASSR and its attentional modulation*

594 We inspected the hemispheric lateralization of the ASSR and its attentional modulation at sensor level using the ASSR
595 power spectrum (obtained in *Methods* 2.5.3 before averaging across all sensors). The ASSR power spectrum was averaged
596 across all gradiometer sensors within each hemisphere, to give the average ASSR power spectrum per hemisphere for each
597 participant. The ASSR power (all units are in T^2/m^2) at $f_m = 41$ Hz corresponding to the Middle voice, irrespective of Attend
598 condition, was extracted for each hemisphere as an objective measure of the raw ASSR signal without the influence of
599 selective attention. In line with previous findings^{25, 43-45}, the ASSR power difference between Right ($M = 4.44 \cdot 10^{-26}$, SD_{bottom}
600 $= 4.2 \cdot 10^{-26}$) and Left hemisphere ($M = 2.36 \cdot 10^{-26}$, $SD_{\text{bottom}} = 2.7 \cdot 10^{-26}$;) yield significant differences ($t(27) = 3.76$, $p_{\text{two-tailed}} <$
601 0.001), demonstrating a Right-hemispheric lateralization of the ASSR. To check the lateralization of the ASSR attentional
602 modulation, for each hemisphere, we extracted the ASSR power at f_m for the Bottom and Top voices per Attend condition.
603 There was no significant hemispheric difference in ASSR attentional modulation for either the voices ($t(27) = 1.15$, $p_{\text{two-}}$
604 $\text{tailed, bottom} = 0.26$; $t(27) = 1.05$, $p_{\text{two-tailed, top}} = 0.30$).

CRedit author statement

Cassia Low Manting: Conceptualization, Methodology, Software, Formal analysis, Investigation, Writing – Original Draft, Writing – Review & Editing, Visualization.

Lau M. Andersen: Methodology, Writing – Review & Editing, Software, Supervision

Balazs Gulyas: Writing – Review & Editing, Supervision, Project administration, Funding acquisition.

Fredrik Ullén: Conceptualization, Methodology, Writing – Review & Editing, Supervision

Daniel Lundqvist: Conceptualization, Methodology, Investigation, Resources, Data Curation, Writing – Review & Editing, Supervision, Project administration, Funding acquisition.

Journal Pre-proof